Phorbol Myristate Acetate Stimulates Microtubule and 10-nm Filament Extension and Lysosome Redistribution in Mouse Macrophages

LINDA PHAIRE-WASHINGTON, SAMUEL C. SILVERSTEIN, and EUGENIA WANG
Carver Research Laboratories, Tuskegee Institute, Tuskegee, Alabama 36088, and Departments of Cellular Physiology and Immunology and of Virology, The Rockefeller University, New York 10021

ABSTRACT Phorbol myristate acetate (PMA) stimulates cell spreading and fluid-phase pinocytosis in mouse peritoneal macrophages. Colchicine (10^{-5} M) and cytochalasin B (10^{-5} M) abolish PMA stimulated pinocytosis but have little effect on cellular spreading (Phaire-Washington et al., 1980, *J. Cell Biol.*, 86:634–640). We report here that PMA also alters the organization of the cytoskeleton and the distribution of organelles in these cells.

Neither control nor PMA-treated macrophages contain actin cables. PMA-treated resident and thioglycolate-elicited macrophages exhibit beneath their substrate-adherent membranes many randomly distributed punctate foci that stain brightly for actin. The appearance and distribution of these actin-containing foci are not altered by colchicine (10^{-5} M) or cytochalasin B (10^{-5} M). In thioglycolate-elicited macrophages PMA causes the extension and radial organization of microtubules and 10-nm filaments and promotes the movement of secondary lysosomes from their perinuclear location to the peripheral cytoplasm. Depending upon the concentration of PMA used, 45–71% of thioglycolate-elicited macrophages and 32–44% of proteose-peptone-elicited macrophages and numerous lysosomes, radiating from the centrosphere region, arranged linearly along microtubule and 10-nm filament bundles. Colchicine (10^{-5} M) and podophyllotoxin (10^{-5} M) prevent the radial redistribution of microtubules, 10-nm filaments, and lysosomes in these cells. Cytochalasins B and D (10^{-5} M) have no inhibitory effects on these processes. These findings indicate that microtubules and 10-nm filaments respond in a coordinated fashion to PMA and to agents that inhibit microtubule function; they suggest that these cytoskeletal elements regulate the movement and distribution of lysosomes in the macrophage cytoplasm.

Compounds that inhibit the function of cytoskeletal proteins, such as cytochalasins and colchicine, cause rounding retraction from the monolayer of a variety of cultured cells, including macrophages (13). In studying the stimulatory effects of the tumor promotor phorbol myristate acetate (PMA) on pinocytosis in mouse macrophages, we noted that PMA induced spreading of the macrophages on the surface of the culture dish (25). Cytochalasin B or colchicine abolished the pinocytosis-stimulating effect of PMA on these cells but had little or no inhibitory effect on cell spreading (25). However, when PMA-treated macrophages were incubated in medium containing both cytochalasin and colchicine, they became more spherical. These findings suggested that PMA stimulates both microtubule- and microfilament-dependent systems, and that the integrity of both systems is required to achieve an increase in pinocytic rate. To further explore these issues, we have examined the effects of PMA on the distribution of actin, tubulin, and 10-nm filaments in mouse macrophages by immunocytochemical methods. Preliminary accounts of this work have been presented (37).

MATERIALS AND METHODS

Cells

Resident, proteose-peptone-elicited, and thioglycolate-elicited mouse peritoneal macrophages were harvested and maintained in culture as described (25).

THE JOURNAL OF CELL BIOLOGY · VOLUME 86 AUGUST 1980 641–655

Published August 1, 1980

Chemicals

PMA (Consolidated Midland Corp., Brewster, N. Y.) at a concentration of 10 mg/ml in dimethylsulfoxide was stored at −70°C in the dark. To prevent repeated thawing, this PMA solution was stored in 25-μl aliquots that were thawed and diluted immediately before use in Eagle's Minimal Essential Medium (MEM) (6) containing 0.1% bovine serum albumin (MEM-BSA). Horseradish peroxide (HRP) type II, cytochalasins B and D, and colchicine were obtained from Sigma Chemical Corp., St. Louis, Mo. Podophyllotoxin and VP-16-213 were gifts from Dr. John Loike of The Rockefeller University.

Cytochemical Localization of Peroxidase and Acid Phosphatase

For light microscopic cytochemistry 1×10^6 peritoneal cells were plated in 35-mm plastic tissue-culture dishes (Falcon Labware, Div. Becton, Dickinson & Co., Oxnard, Calif.) containing .5-inch-diameter glass coverslips. For electron microscopy, the cells were plated on the plastic. The cells were cultured for 24 h in MEM containing 20% fetal bovine serum (MEM-FBS) before use. For peroxidase cytochemistry, the cells were incubated (as indicated in the text and figure legends) in medium containing 1 mg/ml HRP, washed four times with MEM, and fixed for 15 min at room temperature in 2.5% glutaraldehyde in 0.1 M sodium cacodylate buffer (pH 7.4). HRP was visualized by incubating the cells for 30 min at room temperature in the diaminobenzidine- and H_2O_2-containing buffer described by Graham and Karnovsky (10). Coverslip cultures were washed with phosphate-buffered saline and mounted on glass slides for light microscopy. For electron microscopy, macrophages on plastic petri dishes were postfixed for 10–15 min at 4°C with 1% OsO_4 in 0.1 M cacodylate buffer, processed and embedded as described (11), and examined in a Philips 300 electron microscope.

For acid phosphatase cytochemistry, coverslip cultures were fixed in 2.5% glutaraldehyde in 0.1 M cacodylate buffer and processed as described by Cohn and Benson (4).

Preparation of antiserum to various components of cytoskeleton

Antiserum to 10-nm filament proteins was prepared according to the method described by Starger et al. (31). Baby hamster kidney (BHK) cells were treated with colchicine (10 μg/ml) for 24 h. These cells were then used for purification of 10-nm filament proteins. Juxtanuclear caps isolated from these cells contained

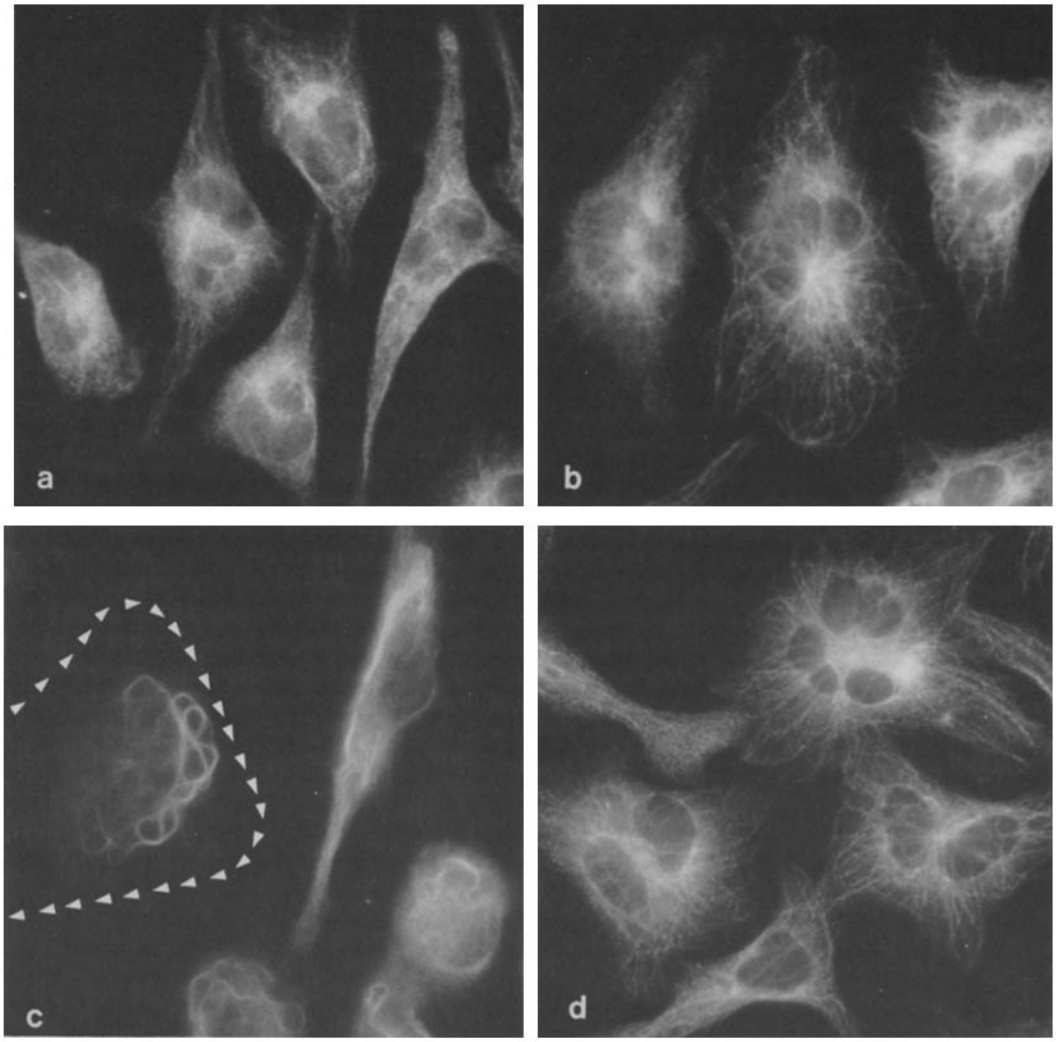

FIGURE 1 Microtubule organization in control and PMA-treated macrophages. Resident and thioglycolate macrophages maintained for 24-h in culture were incubated for 90 min at 37°C in MEM-FBS. Where indicated PMA (0.01 μm/ml) was added to the culture medium. The cultures were then washed, fixed, stained with antitubulin antibodies, and examined by fluorescence microscopy. (*a*) Resident macrophages. (*b*) Resident macrophages treated with PMA. Note the extent of macrophage spreading and the enhanced number of microtubules in the peripheral cytoplasm. (*c*) Thioglycolate macrophages. Microtubules are organized predominantly in bundles that surround the nucleus and, in some cells (center right), extend into the peripheral cytoplasm. The location of the plasma membrane in the cell at left center is marked by arrowheads. This cell is well spread but has no microtubules evident in its peripheral cytoplasm. (*d*) Thioglycolate macrophages treated with PMA. Note the extent of macrophage spreading and the radial arrangement of microtubules. *a–d*, × 1,100.

Published August 1, 1980

a major protein doublet band (mol wt 55,000, 54,000) and a minor high-molecular-weight protein band (>250,000) when analyzed on SDS gels. The juxtanuclear caps were used as the antigen for immunization of rabbits. 4 wk after the initial intramuscular injection (100 μg), two consecutive intravenous injections, 5 d apart, of 50 μg of protein were administered to the rabbits. Antiserum to 10-nm filaments was obtained 3 d after the last boost of antigen. This antiserum was used at a 1:20 dilution for indirect immunofluorescence microscopy. Because rabbits may have "natural" antibodies to 10-nm filaments, preimmune sera from all three rabbits used in antiserum production were examined. No staining of 10-nm filaments were detected using preimmune serum. Adsorption of the anti–10-nm filament serum with 10-nm filament protein inhibited its activity in the fluorescent-staining assay, whereas adsorption of the antiserum with 6S tubulin purified from calf brain did not diminish the staining reaction. This antiserum reacts with 10-nm filaments from a variety of cell types, including BHK-21 fibroblasts, chick embryo fibroblasts, L cells, interferon-treated human fibroblasts, and mouse peritoneal macrophages (Fig. 8).

Cytoplasmic microtubules were visualized by fluorescent antibody staining of tubulin. The specificity of antiserum to 6S calf brain tubulin has been described (34). Actin localization studies were preformed by incubating samples with DNase I in combination with antiserum to DNase I as described by Wang and Goldberg (35).

IMMUNOFLUORESCENCE MICROSCOPY: Cells were plated and maintained on no. 1 glass coverslips, treated as indicated in the figure legends and text, rinsed briefly in phosphate-buffered saline (PBS) at 37°C, fixed in 3.7% formaldehyde in PBS for 30 min at room temperature, rinsed with PBS, immersed in absolute acetone at −20°C for 2 min, and subsequently rinsed in PBS. All following steps, including incubation with antisera and rinsing with PBS, were conducted at 37°C. Coverslips were drained, overlaid with 50 μl of a 1:20 dilution of the appropriate rabbit antiserum, incubated for 30 min in a humid chamber, rinsed in PBS, and incubated for 30 min with 50 μl of fluorescein-conjugated goat antirabbit IgG at a protein concentration of 0.5 mg IgG per ml. The coverslips were rinsed in PBS and mounted on glass slides for microscopy in a medium composed of equal parts of glycerol and PBS. (To reduce the nonspecific background staining, the second antibody was absorbed with formaldehyde-fixed and acetone-treated cells, and centrifuged at 10,000 rpm for .5 h before being used.)

The cells were examined with a Zeiss photomicroscope equipped with epifluorescence optics. Photomicrographs were taken with a phase 3 (63/1.4 objective), using Kodak Tri-X pan film with an ASA rating of 1600. Fluorescence exposure times were 1–1.5 min.

ELECTRON MICROSCOPY: Cells were plated in 35-mm plastic tissue-culture dishes, treated as appropriate, fixed for 30 min at room temperature in 1% glutaraldehyde in PBS (pH 7.4), postfixed for 30 min in 1% OsO_4 (pH 7.4), dehydrated in graded ethanol series, and embedded in Epon 812 (23). Serial 500–600 Å thick sections, beginning at the substrate-adherent cell surface, were cut parallel to the plane of cell attachment. Sections were doubly stained with hot uranyl acetate in 95% ethanol (21) and lead citrate (26), examined in a Philips 300 electron microscope.

RESULTS

PMA Induces Reorganization of Microtubules

Resident macrophages contain a modest number of microtubules radiating from the centrosphere (Fig. 1 *a*). After PMA treatment, the pattern of microtubule staining is qualitatively unchanged but the number of tubules radiating into the peripheral cytoplasm appears to be increased (Fig. 1 *b*). Whether

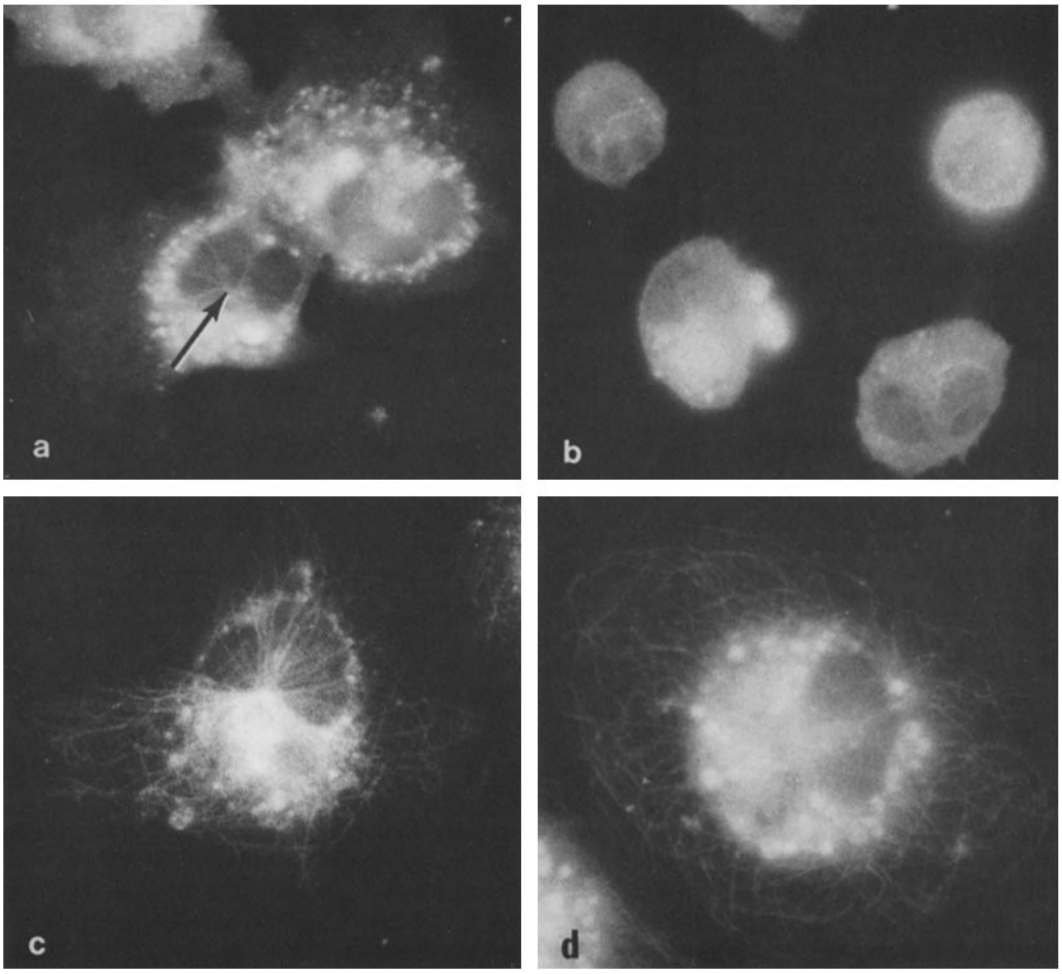

FIGURE 2 Effects of colchicine, podophyllotoxin, and cytochalasin B on microtubule organization of PMA-treated thioglycolate macrophages. Cells maintained in culture for 24 h were incubated for 90 min at 37°C in MEM-FBS containing PMA (0.01 μg/ml) and the indicated drug, and processed as described in Fig. 1. (*a*) Colchicine, 10^{-5} M. Some perinuclear microtubules (arrow) remain intact even at this dose of colchicine. (*b*) Podophyllotoxin, 10^{-5} M. (*c*) VP-16-213, 10^{-5} M. (*d*) Cytochalasin B, 10^{-5} M. *a* and *b*, × 850. *c*, × 1,000. *d*, × 1,100.

Published August 1, 1980

this is a cause or a result of PMA-induced cell spreading is unresolved.

Thioglycolate-elicited macrophages labeled with antitubulin antibodies demonstrate striking changes in the intracellular organization of microtubules after PMA treatment (Fig. 1 *c* and *d*). In untreated thioglycolate-elicited macrophages, antitubulin staining is concentrated in bundles that surrounded the nucleus and the centrosphere region (Fig. 1 *c*). Some exceptionally well spread cells show a network of microtubules in the peripheral cytoplasm as well (Fig. 1 *c*). After PMA treatment,

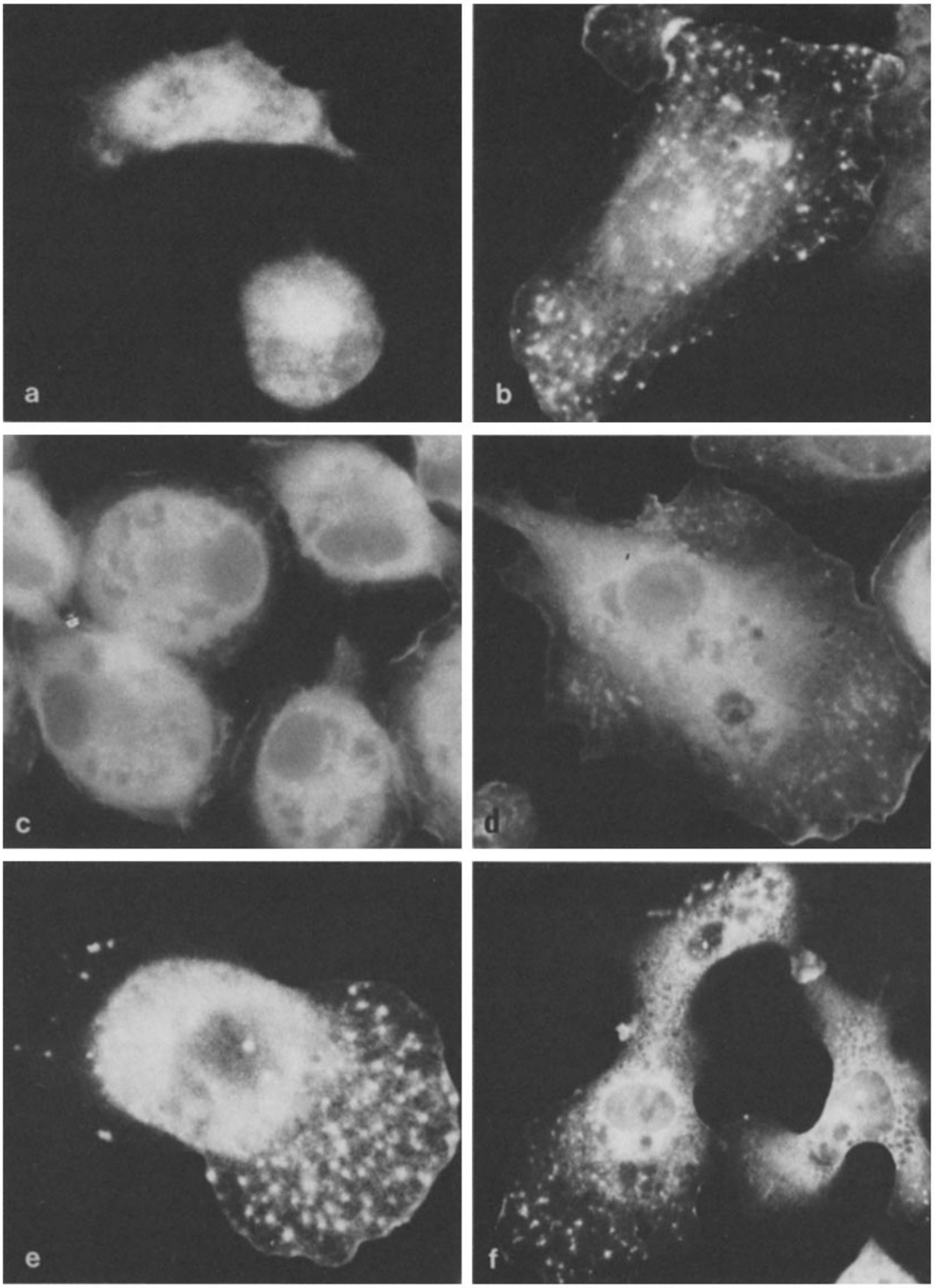

FIGURE 3 Distribution of cytoplasmic actin in control and PMA-treated macrophages. Resident and thioglycolate macrophages maintained for 24 h in culture were incubated for 90 min at 37°C in MEM-FBS. Where indicated, PMA (0.01 μg/ml) and colchicine (10^{-5} M) were added to the culture medium. The cultures were then washed, fixed, incubated with DNase and fluorescein-labeled anti-DNase to stain actin-containing structures, and examined by fluorescence microscopy. (*a*) Resident macrophages. (*b*) Resident macrophages treated with PMA. Note the extent of cell spreading and the punctate accumulations of actin throughout the cytoplasm. (*c*) Thioglycolate macrophages. (*d*) Thioglycolate macrophages treated with PMA. (*e*) Resident macrophage treated with PMA and colchicine. (*f*) Thioglycolate macrophages treated with PMA and colchicine. *a* and *b*, 1,200. *c*–*e*, × 1,000. *f*, × 500.

Published August 1, 1980

the macrophages spread circumferentially on the substrate (25). Antitubulin staining of these PMA-treated cells reveals a well-organized, radially arranged network of microtubules that emanates from the centrosphere and extends into the peripheral cytoplasm (Fig. 1 *d*). Electron microscope analysis confirms these immunofluorescent observations. Increased numbers of microtubules are seen both in the centrosphere region and in the peripheral cytoplasm of PMA-treated, thioglycolate-elicited macrophages (cf Fig. 11 *a* and *b*).

TABLE I

PMA-induced Redistribution of Peroxidase-containing Granules *

	Percentage of cells with radially arrayed granules	
PMA	Thioglycolate macrophages	Proteose-peptone macrophages
μg/ml		
0	5	4
0.001	52	37
0.005	65	ND
0.01	71	44
0.1	60	38
1.0	54	32
10.0	45	ND

* Thioglycolate-elicited, or proteose-peptone-elicited macrophages, maintained in culture for 24 h, were incubated for 1 h at 37°C in MEM containing 1 mg/ml HRP and PMA as indicated. The cells were then washed, fixed, and stained to localize intracellular peroxidase, as described in Materials and Methods, and examined by phase microscopy. The percentage of cells on each coverslip containing radially aligned peroxidase-containing granules was determined. Cells were considered to exhibit redistribution of their peroxidase-containing granules if they contained at least three radially aligned arrays of peroxidase-stained granules that originated in the centrosphere and extended into the peripheral cytoplasm. At least 100 cells were counted on each coverslip. *ND*, not determined.

Addition of colchicine (10^{-5} M) or podophyllotoxin (10^{-5} M) to the medium, either before or after PMA treatment of resident (not shown) or thioglycolate-elicited macrophages, causes the disappearance of microtubule staining in the peripheral cytoplasm (Fig. 2 *a* and *b*). VP-16-213, an analog of podophyllotoxin that lacks tubulin-binding activity (22), and cytochalasin B have no effect on the microtubule staining pattern of control (not shown) or PMA-treated thioglycolate macrophages (Fig. 2 *c* and *d*).

Cytochalasin D (10^{-5} M) has a pronounced effect on the appearance of the plasma membranes of PMA-treated thioglycolate macrophages. These cells exhibit an arborized appearance (Fig. 7 *b*), but microtubules remain evident in their distorted membrane projections (not shown).

PMA Induces Changes in the Fluorescent-staining Patterns of Cytoplasmic Actin

The organization of cytoplasmic actin was examined by indirect immunofluorescent staining with DNase and fluorescein-labeled anti-DNase. By this method, resident and thioglycolate-elicited macrophages are diffusely stained throughout their cytoplasm and along their membrane periphery (Fig. 3 *a* and *c*). There are no actin cables. After PMA treatment, actin-rich patches appear randomly scattered throughout the cytoplasm (Fig. 3 *b* and *d*). This PMA-induced alteration in the distribution of cytoplasmic actin is not inhibited by colchicine (Fig. 3 *e* and *f*). Macrophages treated with PMA and cytochalasin B (10^{-5} M) exhibit a similar actin staining pattern at their cell margins but show fewer actin-rich patches than cells treated with PMA alone, whereas macrophages treated with PMA and cytochalasin D (10^{-5} M) have none of these actin-rich patches (not shown). Virtually all of the PMA-induced actin-rich

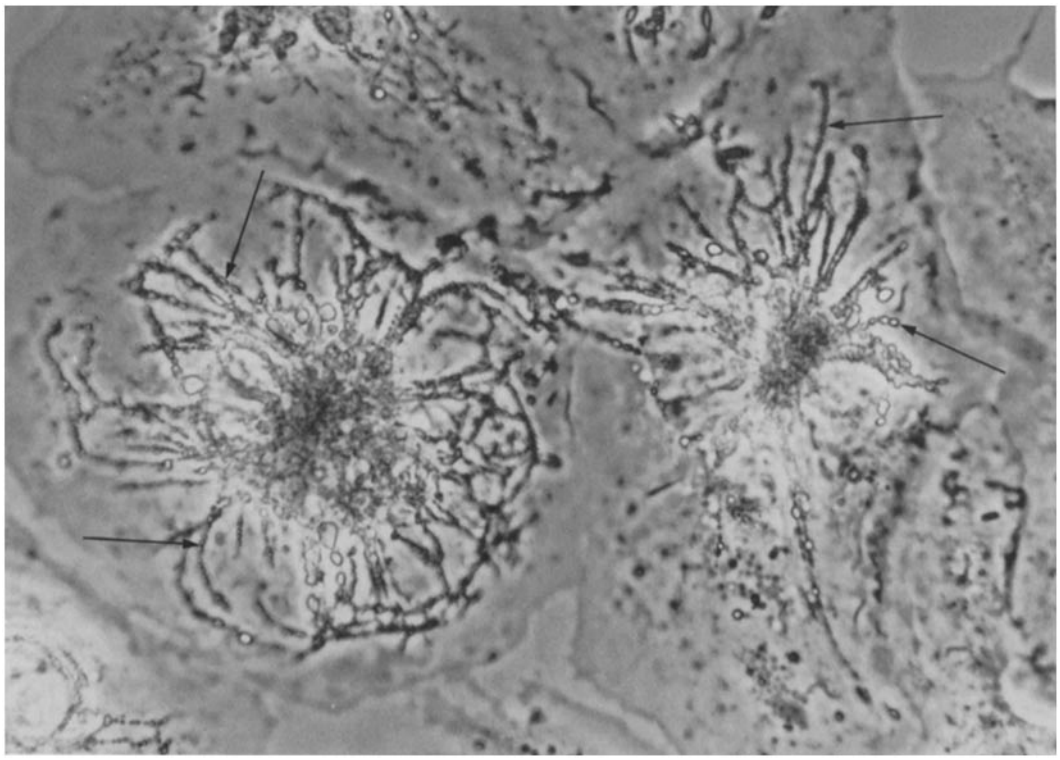

FIGURE 4 Cytochemical localization of peroxidase in PMA-treated thioglycolate macrophages. 24-h explanted macrophages were incubated in medium containing peroxidase and PMA (0.01 μg/ml) and processed as described in Table I legend. Arrows point to chains of peroxidase-stained granules. × 2,940.

Published August 1, 1980

patches are concentrated on the macrophages' glass-adherent membrane surfaces. In the absence of PMA, well-spread macrophages do not contain these actin-rich patches. For this reason, we think that spreading alone cannot account for the appearance of actin-rich patches.

PMA Induces the Radial Alignment of Secondary Lysosomes

Thioglycolate- or proteose-peptone-elicited macrophages were incubated with PMA and HRP for 15–60 min at 37°C. The cells were then fixed, stained for peroxidase, and examined by light and electron microscopy. Depending upon the concentration of PMA used, 45–71% of thioglycolate-elicited macrophages and 32–44% of proteose-peptone-elicited macrophages had numerous peroxidase-labeled granules radiating in longitudinal arrays from the centrosphere (Table I and Fig. 4). In the absence of PMA, <6% of the macrophages exhibited any of these radially arranged peroxidase-stained granules (Table I). Macrophages incubated in PMA alone showed no peroxi-

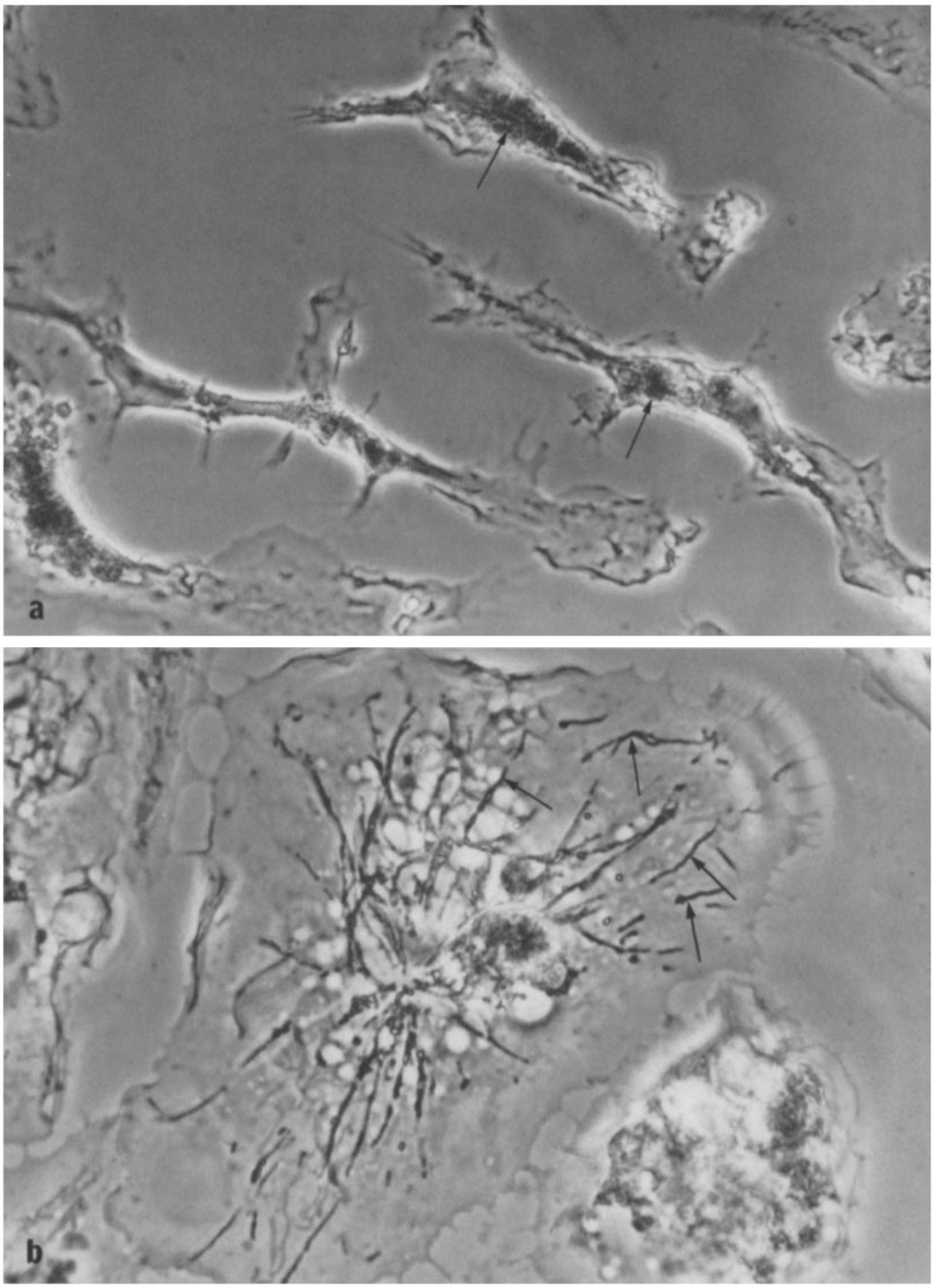

FIGURE 5 Cytochemical localization of acid phosphatase in (*a*) control and (*b*) PMA-treated thioglycolate macrophages. 24-h explanted macrophages were incubated for 60 min at 37°C in MEM-FBS. PMA (0.01 μg/ml) was added to the medium of the cells shown in panel *b*. Arrows indicate granules stained positively for acid phosphatase. *a*, × 2,000. *b*, × 3,500.

Published August 1, 1980

dase staining, confirming that the diaminobenzidine-stained granules reflect peroxidase endocytosed from the medium.

Steinman et al. (32) showed that HRP is concentrated within macrophage lysosomes within 5 min of its uptake by pinocytosis. Thus, it seemed likely that most of the peroxidase-stained granules in PMA-treated cells were secondary lysosomes. We therefore examined the distribution of acid phosphatase-containing granules in these cells. PMA-treated macrophages contain linear arrays of acid-phosphatase-stained granules radiating from the centrosphere region in the same distribution as the peroxidase-stained granules (cf. Figs. 4 and 5*b*). Macrophages maintained in the absence of PMA have their acid-phosphatase-containing granules concentrated in the perinuclear area (Fig. 5*a*). Electron microscopy of macrophages incubated with PMA and peroxidase and stained with diaminobenzidine, showed that the peroxidase was contained in electron-dense oblong structures bound by a single unit membrane. These granules were close to parallel arrays of micro-

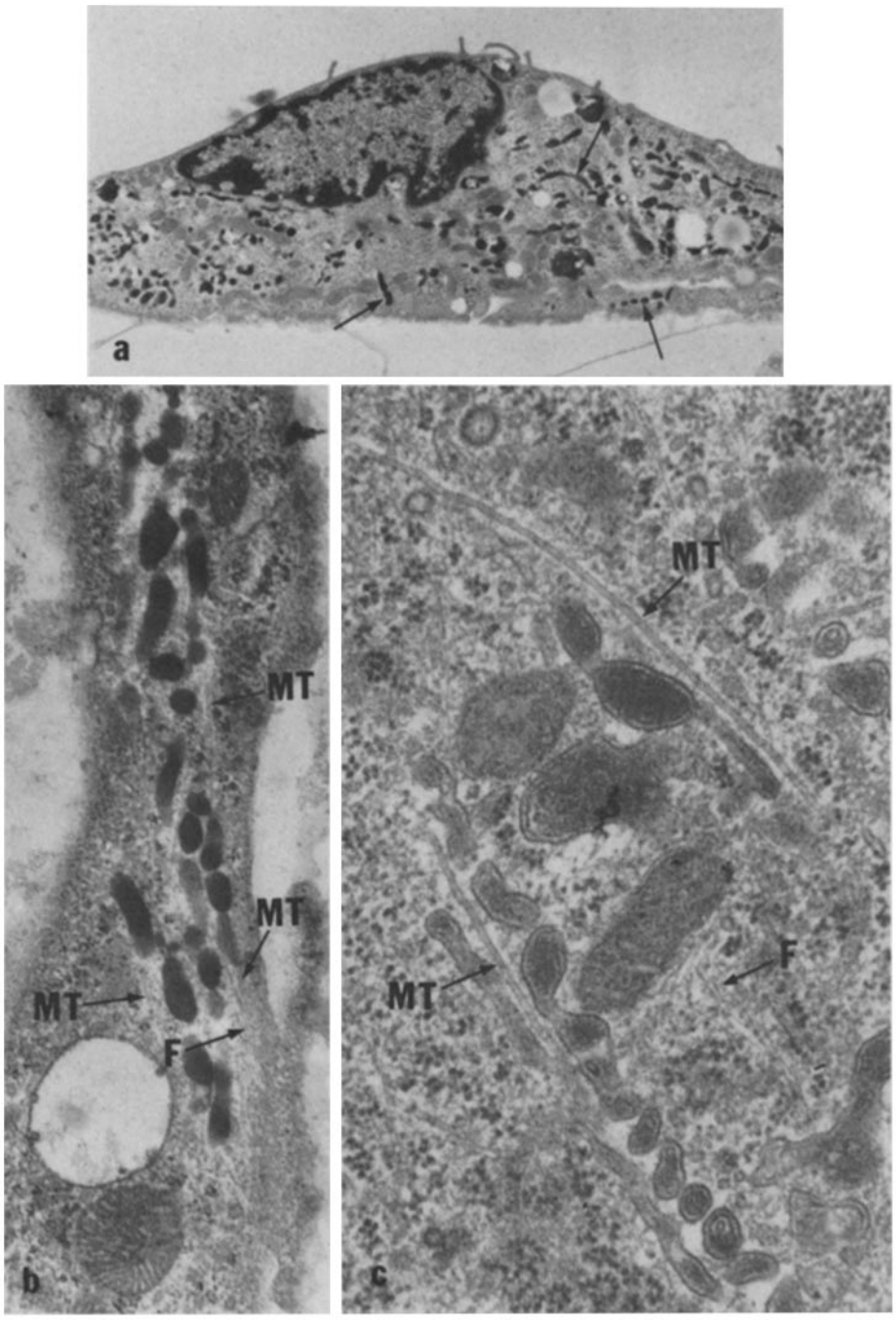

FIGURE 6 Ultrastructural localization of peroxidase in PMA-treated thioglycolate macrophages. Protocol was identical to that in Fig. 4, except that the cells were plated and processed for electron microscopy as described in Materials and Methods. (*a*) Section through cell body showing many chains of peroxidase-stained granules (arrows). (*b*) Section through peripheral cytoplasm showing parallel arrays of peroxidase-stained granules in association with microtubules (*MT*) and 10-nm filaments (*F*). (*c*) Similar to panel *b*, except that the cells in this culture were processed directly for electron microscopy without prior incubation in diaminobenzidine-containing medium. Granules are aligned along microtubules (*MT*). a, × 6,500. b, × 16,240. c, × 41,600.

Published August 1, 1980

tubules and 10-nm filaments (Fig. 6 *a*, *b*, and *c*). We conclude that the peroxidase- and acid-phosphatase-stained granules found in linear arrays in PMA-treated macrophages are secondary lysosomes.

To determine the direction of movement of peroxidase-containing lysosomes after PMA stimulation, thioglycolate macrophages were incubated in HRP for 15–60 min. Some of these cultures were fixed and stained for peroxidase. Virtually all their peroxidase-stained granules were in the perinuclear area. Another group of cultures was washed to remove the peroxidase from the medium, incubated for 15–60 min in PMA-containing (0.01 μg/ml) medium, fixed, and stained for peroxidase. 50–60% of these cells showed linear arrays of peroxidase-containing granules radiating from the centrosphere region. The number and intensity of staining of these granules was dependent upon the time the cells were incubated in HRP, but was independent of whether the macrophages were treated with PMA for 15 min or longer. Thus, peroxidase-labeled lysosomes in the centrosphere region are rapidly transported to the cell's periphery after PMA treatment.

To examine the mechanism of lysosomal translocation, macrophages were incubated with peroxidase and PMA for 1 h, and further incubated for 30 min with colchicine, podophyllotoxin, VP-16-213, cytochalasin B or cytochalasin D. Colchicine and podophyllotoxin each caused retraction of the peroxidase-stained granules into the perinuclear area (Fig. 7 *a* and Table II), whereas VP-16-213 (Table II) and cytochalasins B and D caused no measurable decrease in the number of cells with linear arrays of peroxidase-stained granules radiating into the peripheral cytoplasm (Fig. 7 *b* and Table III). In a parallel series of experiments, thioglycolate macrophages were incubated with peroxidase in the absence of PMA, and then further incubated in medium containing PMA. Colchicine (10^{-5} M) or cytochalasin B (10^{-5} M) was added to some of the cultures at the same time as PMA. Cells treated with PMA alone, or with PMA and cytochalasin B, showed equal numbers of linearly arrayed peroxidase-containing granules; cells treated with PMA and colchicine retained their peroxidase-containing granules in the perinuclear area. Thus, cytochalasin B had no measurable inhibitory effect on either the movement of peroxidase-containing lysosomes from the centrosphere region to the peripheral cytoplasm, or on their maintenance in this location. In contrast, colchicine inhibited the cell's capacity to transport these lysosomes out of the centrosphere region, and promoted their return to the perinuclear zone.

These findings indicate that cytoskeletal elements whose distribution is altered by colchicine are principally responsible for the PMA-induced movement of secondary lysosomes in the macrophage cytoplasm. Wang and Goldman (36) have shown that colchicine disrupts the organization of microtubules and 10-nm filaments, and inhibits the saltatory movement of organelles in BHK-21 cells. Therefore, we examined the distribution of 10-nm filaments in control and PMA-treated macrophages.

Immunofluorescence microscopy showed that in resident and thioglycolate macrophages, 10-nm filaments were concentrated on the perinuclear region and exhibit a random, swirling pattern (Fig. 8 *a* and *c*).10-nm filaments also appeared in bundles encircling membranous vacuoles. Some cells had fluorescent fibers extending into their cytoplasmic processes. Resident macrophages treated with PMA showed only a small increase in the number of 10-nm filaments in their peripheral cytoplasm (Fig. 8 *b*). In contrast, PMA-treatment of thioglycolate macrophages induced a marked redistribution of 10-nm filaments from the perinuclear region to the peripheral cytoplasm (cf. Fig. 8 *c* and *d*). The 10-nm filaments in the peripheral cytoplasm had a radial distribution, except at the cell margins where some of these fibers coursed circumferentially (Fig. 8 *d*).

The organization of 10-nm filaments in the peripheral cytoplasm corresponded closely to the distribution of microtubules

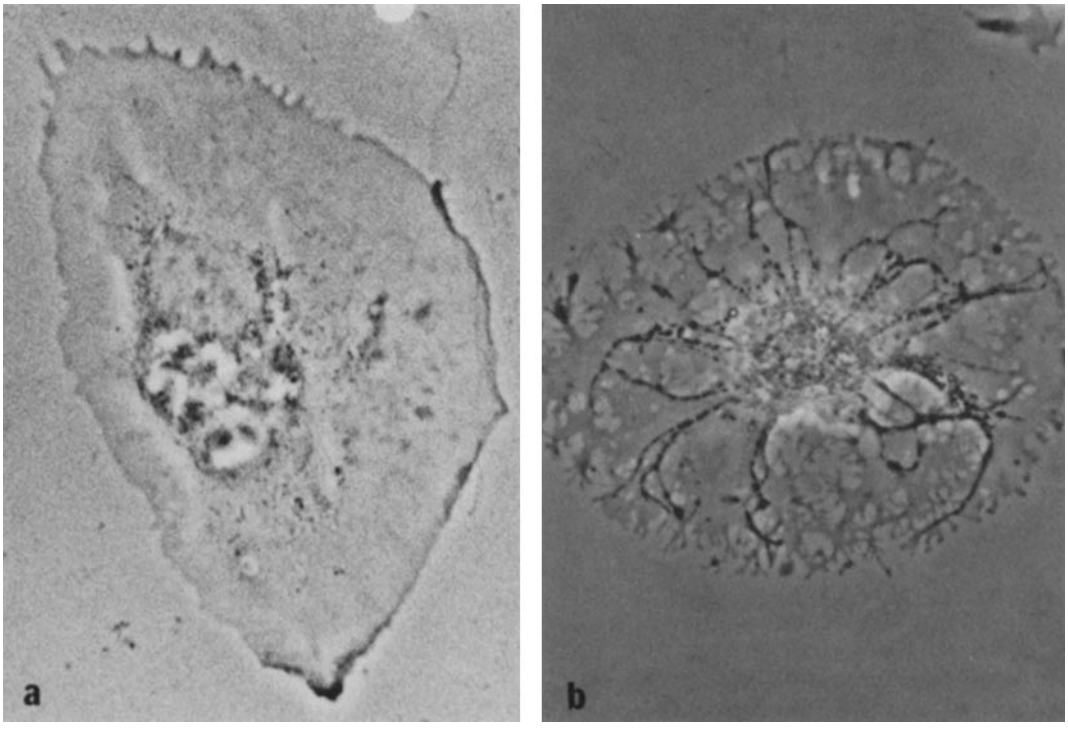

FIGURE 7 Cytochemical localization of peroxidase in thioglycolate macrophages incubated in horseradish peroxidase and PMA (0.01 μg/ml) and subsequently treated with (*a*) colchicine or (*b*) cytochalasin D. Experimental protocol is the same as that described in Tables II and III.

Published August 1, 1980

(Fig. 1 *b*) and lysosomes (Figs. 4 *b* and 5 *b*) in this location. In the centrosphere region, however, microtubules and 10-nm filaments differed from one another in organization. Microtubules radiated from a single site located at the centrioles, whereas 10-nm filaments formed continuous loops and bands that had no single locus of origin.

To examine further the relationship between 10-nm filaments and cytoplasmic organelles, we compared the distribution of mitochondria and 10-nm filaments in the same cells. Phase-contrast microscopy showed that before PMA treatment few of the mitochondria in thioglycolate macrophages were present in the peripheral cytoplasm (Fig. 9 *a*); they were concentrated in the perinuclear region. When the same cells were examined by fluorescence microscopy (Fig. 9 *b*), 10-nm filaments were also concentrated in the perinuclear region.Treatment of these macrophages with PMA induced the movement of mitochondria into the cell processes. The mitochondria assumed a vermiform appearance and were arrayed parallel to each other (Fig. 9 *c*). Examination of the same cells with fluorescence optics showed that bundles of 10-nm filaments extended into the peripheral cytoplasm parallel to the vermiform mitochondria positioned along them (Fig. 9 *d*).

Addition of colchicine to the medium caused the disappearance of microtubules from the peripheral cytoplasm (Fig. 2 *a*), and the retraction of 10-nm filaments (Fig. 10 *b*), mitochondria (Fig. 10 *a*), and lysosomes (Fig. 7 *a*) into the perinuclear region of PMA-treated macrophages. However, no retraction of 10-nm filaments (Fig. 10 *d*), microtubules, mitochondria (Fig. 10 *c*), or lysosomes was noted when cytochalasin E was added to the medium of PMA-treated thioglycolate macrophages. Similar results were obtained with cytochalasins B and D.

The PMA-induced changes in 10-nm filament distribution identified by fluorescence microscopy were confirmed by transmission electron microscopy. Serial thin sections beginning with the substrate-adherent portions of PMA-treated thioglycolate macrophages showed that microtubules were concentrated in the portion of the cytoplasm closest to the culture dish, whereas 10-nm filaments appeared at virtually every level.

In the absence of PMA, mitochondria, lysosomes, and pinocytosis vesicles showed no consistent orientation with regard to microtubules. Individual 10-nm filaments frequently appeared near these organelles (Fig. 11 *a*). In contrast, PMA-treated macrophages revealed an orderly linear arrangement of organelles, microtubules, and 10-nm filaments (Fig. 11 *b*). Mitochondria, coated vesicles, and smooth vesicles were aligned among these parallel arrays of microtubules and 10-nm filaments. The 10-nm filaments were frequently found in bundles in PMA-treated cells, and these 10-nm filament bundles surrounded large membrane-bounded vacuoles. Thus, both fluorescence and electron microscopy showed a parallel distribution of longitudinally arrayed 10-nm filaments and microtubules near the basal surface of PMA-treated macrophages. In addition, bundles of 10-nm filaments unaccompanied by microtubules were seen encircling the centrosphere region and cytoplasmic vacuoles in these cells.

TABLE II

Radial Translocation of Peroxidase-containing Granules Inhibited by Drugs That Alter Microtubule Function *

Macrophage treatment	Percentage of macrophages with radially arrayed peroxidase-containing granules
None	7
PMA (0.1 μg/ml)	47
PMA + colchicine (10^{-5} M)	0
PMA + podophyllotoxin (10^{-5} M)	0
PMA + VP-16-213 (10^{-5} M)	55

* 24-h thioglycolate macrophages were incubated for 60 min at 37°C in medium containing PMA (0.01 μg/ml) and peroxidase (1 mg/ml). Colchicine, podophyllotoxin, or VP-16-213 was added to the cultures for an additional 30 min, after which the cells were washed, fixed, and stained as described in Table I legend to visualize intracellular peroxidase. The percentage of cells with radially arrayed granules was evaluated by light microscopy as in Table I.

TABLE III

Radial Translocation of Peroxidase Not Affected by Cytochalasins B or D *

Macrophage treatment	Percentage of macrophages with radially arrayed peroxidase-containing granules
None	7
PMA	55
PMA + 10^{-5} M Cytochalasin B	49
PMA + 10^{-6} M Cytochalasin B	57
PMA + 10^{-5} M Cytochalasin D	55
PMA + 10^{-6} M Cytochalasin D	60

* Experimental protocol was the same as in Table II, except that cytochalasins B and D were used in place of colchicine, podophyllotoxin, and VP-16-213.

DISCUSSION

The experiments reported here and in a companion paper (25) document that PMA exerts a variety of effects on macrophage morphology and function. Prominent among the effects of PMA on thioglycolate-elicited macrophages are enhanced cellular spreading, redistribution of cytoplasmic actin,[1] extension of parallel arrays of microtubules and 10-nm filaments into the peripheral cytoplasm, orientation of mitochondria and lysosomes along these microtubule and 10-nm filament bundles, and a marked increase in pinocytic rate. We have examined the effects of colchicine, podophyllotoxin, and cytochalasins B and D on each of these PMA-induced alterations in cell structure and functions. In this way we have tried to identify the cytoskeletal elements responsible for a given morphological or functional change and to determine whether any of these changes are causally related to one another. The results of our studies on thioglycolate-elicited macrophages are summarized in Table IV.

A caveat of all drug studies is that unrecognized side effects, unrelated to the primary site of drug action, may be responsible for the changes observed. Because this is a possible pitfall in the present instance, we examined the effects of several compounds or congeners of a single compound. Colchicine and podophyllotoxin produced identical effects, whereas VP-16-213, a podophyllotoxin analog that inhibits nucleoside transport but does not alter microtubule function (22), was inactive. Cytochalasin D is considerably more potent than cytochalasin B in inhibiting both basal and PMA-stimulated pinocytosis (25), and PMA-induced cell spreading, yet it exhibits little or none of the inhibitory effect of cytochalasin B on glucose transport (1) in macrophages (J. Loike and S. Silverstein, unpublished observations). Thus the "side effects" of these compounds on membrane transport systems do not appear responsible for their inhibitory effects. For the remainder of this discussion we assume that colchicine and the cytochalasins

[1] In chick fibroblasts, PMA is reported to cause a decrease in the number of actin cables (27).

inhibit PMA-induced processes by altering microtubule (30) or actin filament (3, 12, 20, 38) functions, respectively.

Effects of PMA on Colchicine-sensitive Cytoskeletal Elements

Goldstein et al. (9) reported that polymorphonuclear leukocytes treated with PMA and cytochalasin B contain increased numbers of microtubules. In the present study we extend their findings to thioglycolate-elicited macrophages (Fig. 2 *d*). In addition, we show that thioglycolate macrophages treated with PMA in the presence or absence of cytochalasins B or D exhibit 10-nm filament extension, translocation of lysosomes from the centrosphere to the peripheral cytoplasm, and alignment of lysosomes and mitochondria along parallel arrays of 10-nm filaments and microtubules (Table III and Figs. 4–11). Cyto-

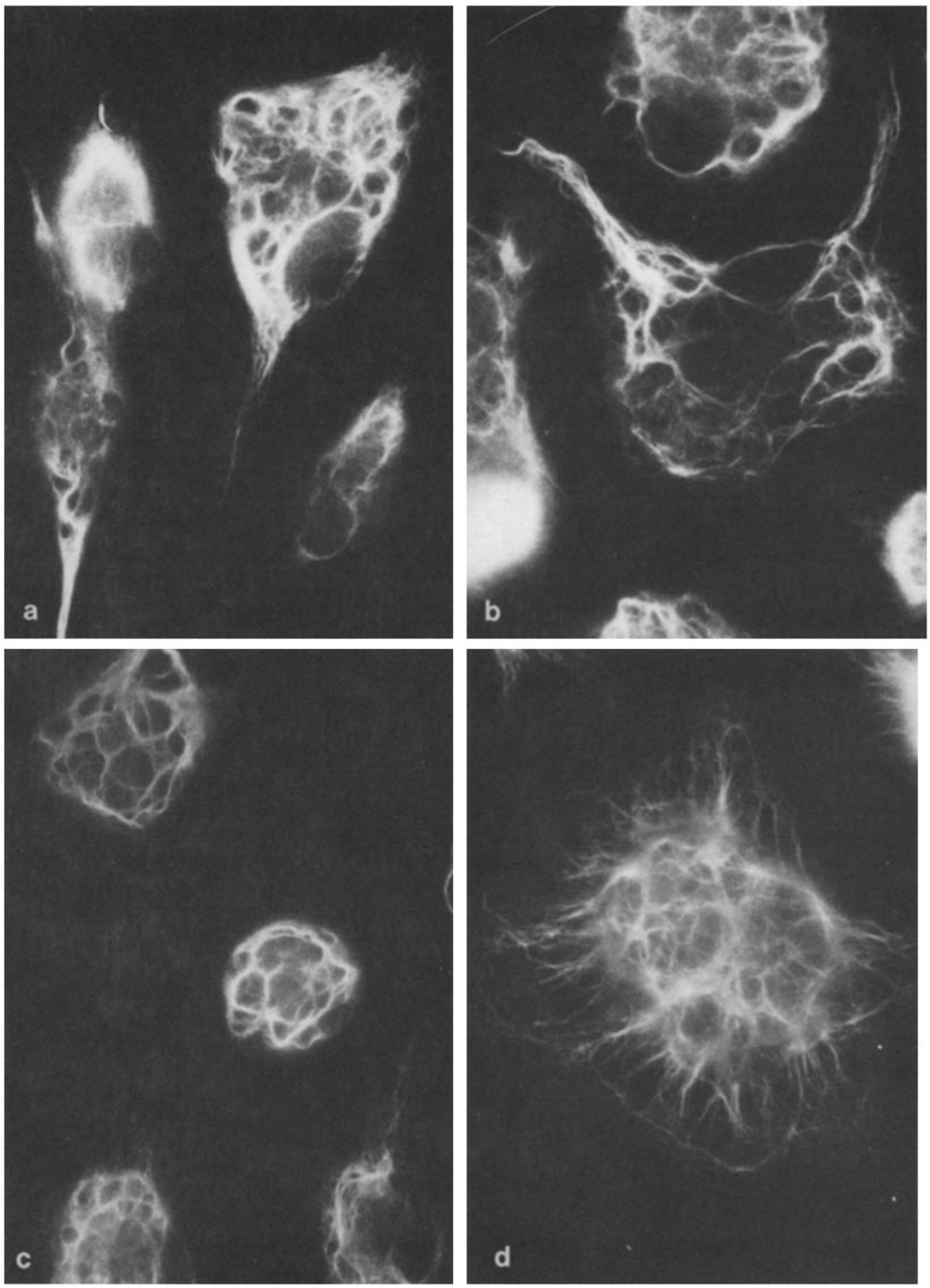

FIGURE 8 Immunofluorescence microscopy of 10-nm filaments in resident and thioglycolate macrophages. Cells were maintained for 24 h in culture before use (*a*) Resident macrophages. (*b*) Resident macrophages treated with PMA (0.01 μg/ml) for 30 min at 37°C before fixation and staining. (*c*) Thioglycolate macrophages. (*d*) Thioglycolate macrophages treated with PMA (0.01 μg/ml) for 30 min at 37°C before fixation and staining. a, × 2,000. b, × 1,000. c, × 1,400. d, × 700.

Published August 1, 1980

chalasin B does not inhibit the movement and the alignment of nuclei along microtubule and 10-nm filament bundles in cytochalasin B–treated, virus-induced syncytia (34). These findings suggest that cytochalasin-sensitive actin filaments are not involved in the movement of nuclei, mitochondria, and lysosomes.

A close anatomical relationship between microtubules and 10-nm filaments is seen in a variety of cell types including neurons, fibroblasts (8, 34, 36), and PMA-treated macrophages (Fig. 11), and Goldman (8) has shown that 10-nm filaments and microtubules react in a coordinated fashion in BHK-21 cells in response to microtubule-disrupting agents. The importance of microtubules in the movement and organization of cytoplasmic organelles is well-documented (2, 5, 15–18, 33). In

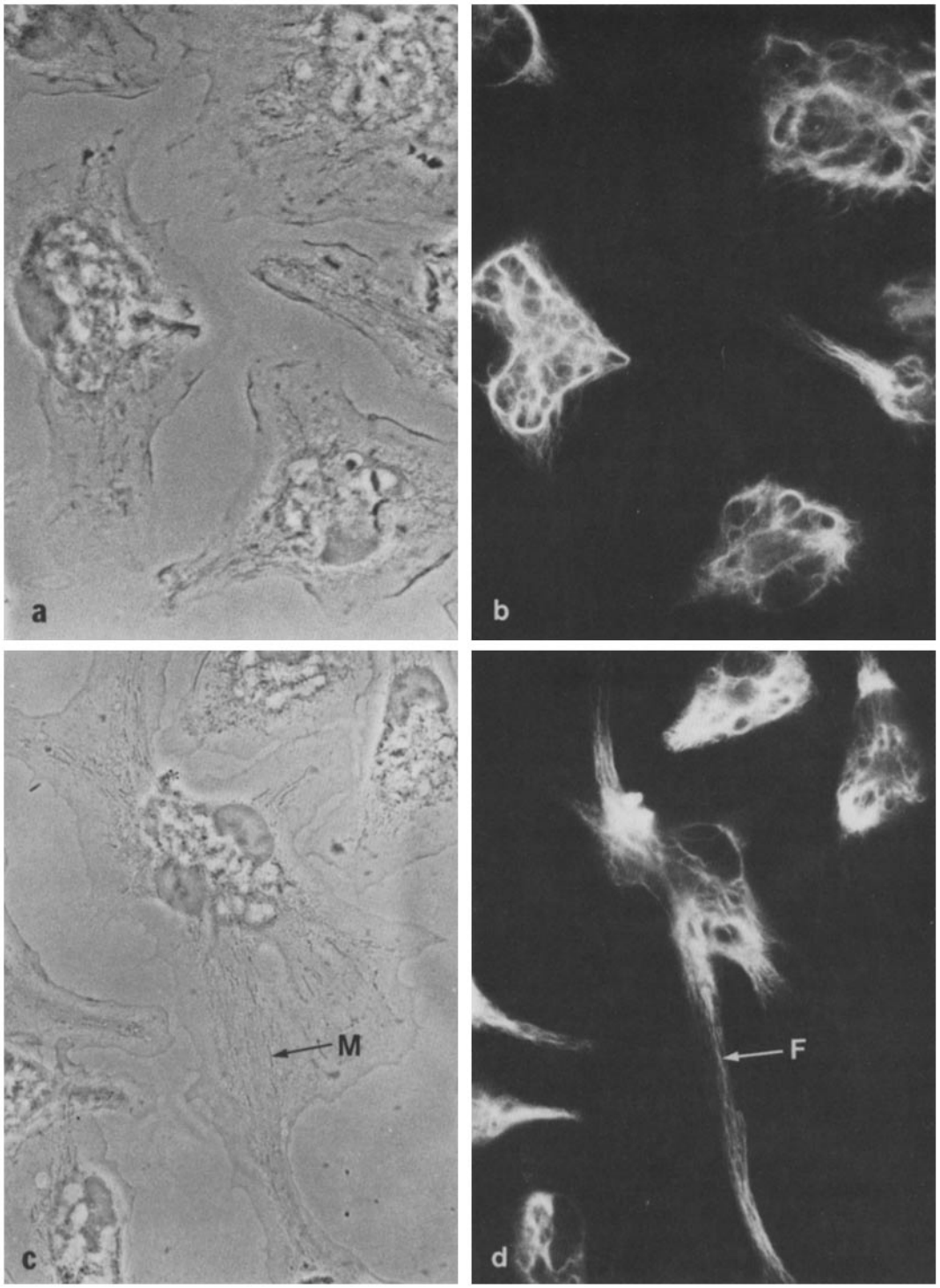

FIGURE 9 Comparison of mitochondrial (*M*) and 10-nm filament (*F*) distribution in control and PMA-treated thioglycolate macrophages. Panels *a* and *c*, phase-contrast microscopy. Panels *b* and *d*, fluorescence microscopy. Panels *a* and *b*, control thioglycolate macrophages. Panels *c* and *d*, thioglycolate macrophages treated with PMA (0.01 μg/ml) for 60 min at 37°C before fixation and staining for 10-nm filaments. × 1,200.

Published August 1, 1980

fibroblasts, mitochondria (36) and nuclei (15, 34) display saltatory movements along parallel arrays of microtubules and 10-nm filaments. The remarkable resemblance between the arrangement of microtubules and 10-nm filaments observed in PMA-treated macrophages and in fibroblasts suggests that these cytoskeletal elements may control the saltatory movements and cytoplasmic location of organelles in both cell types.

Although organelles are aligned along microtubules, there is no evidence that they are in direct contact with them. In contrast, bundles of 10-nm filaments encase the nucleus (Figs. 8 and 9) and surround many cytoplasmic vacuoles, lysosomes, and mitochondria. These findings suggest that 10-nm filaments are the principal cytoskeletal elements controlling organelle movements.

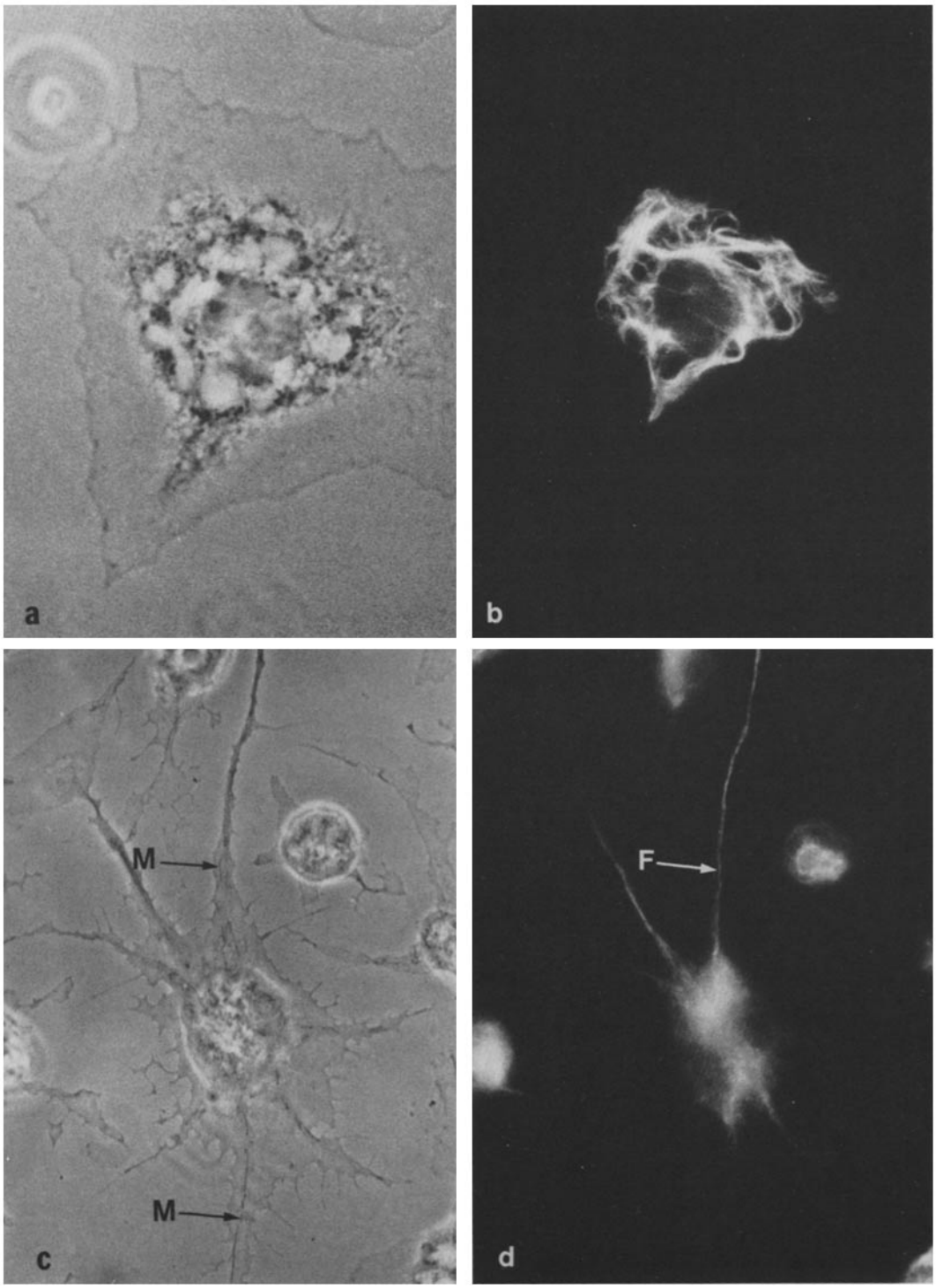

FIGURE 10 Comparison of the distribution of mitochondria (*M*) and of 10-nm filaments (*F*) in thioglycolate macrophages treated with PMA and colchicine or cytochalasin E. Panels *a* and *c*, phase-contrast microscopy. Panels *b* and *d*, fluorescence microscopy. Thioglycolate macrophages were treated with PMA (0.01 μg/ml) for 60 min at 37°C. Colchicine (10^{-5} M) (panels *a* and *b*) or cytochalasin E (10^{-5} M) (panels *c* and *d*) was added to the cultures for an additional 30 min. The cells were then fixed and examined. × 1,400.

Published August 1, 1980

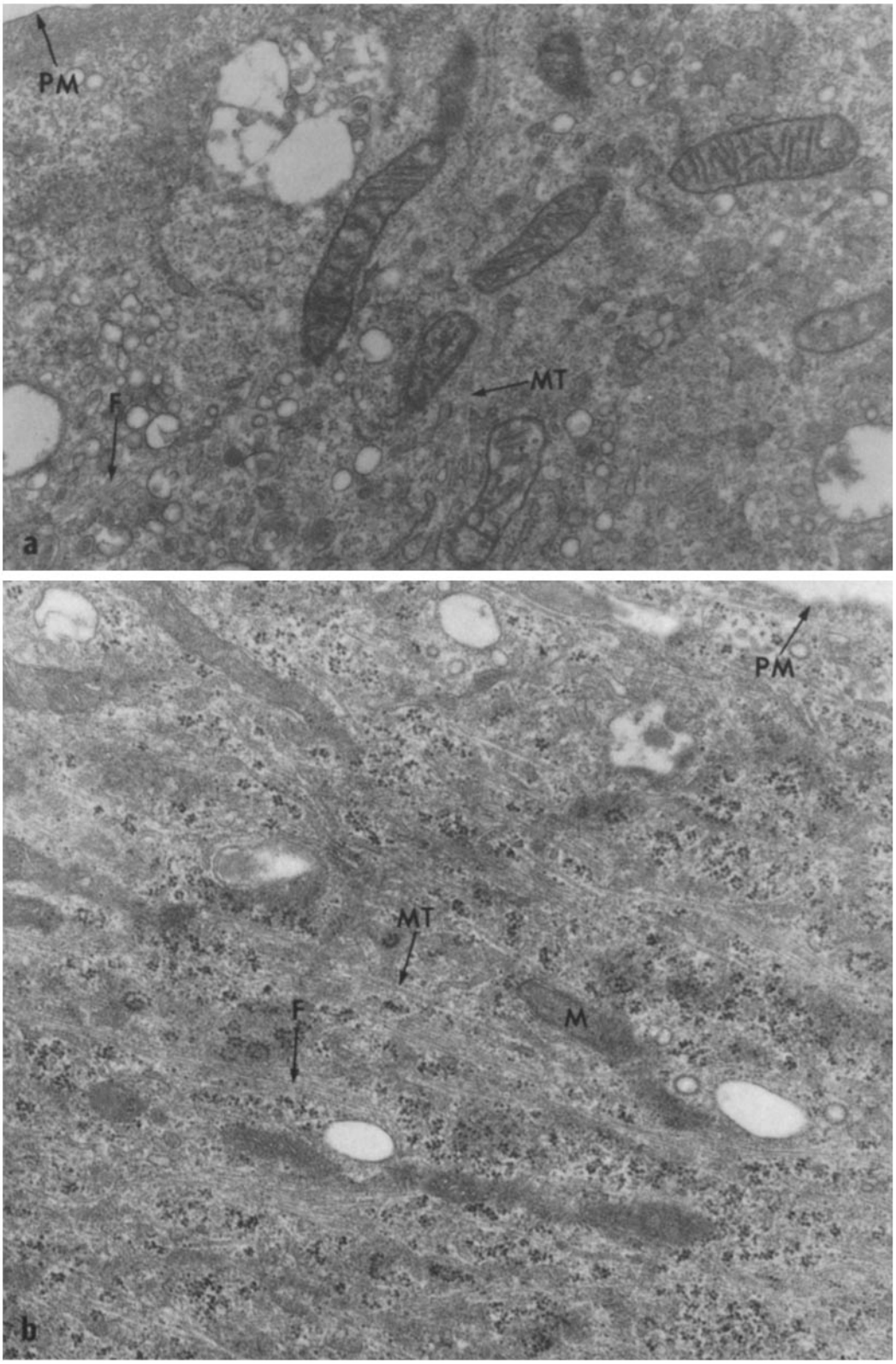

FIGURE 11 Electron micrographs of control and PMA-treated thioglycolate macrophages. Macrophages, maintained in culture for 24 h, were incubated for 1 h in MEM-FBS at 37°C in the absence (*a*) or presence (*b*) of PMA (0.01 μg/ml). Sections shown are close to the cells' basal surface and to the plasma membrane (*PM*). Note the parallel alignment of microtubules (*MT*), 10-nm filaments (*F*), and mitochondria (*M*) in *b*, and not in *a*. a, × 28,300. *b*, × 32,730.

Published August 1, 1980

TABLE IV

Summary of the Effects of PMA, Cytochalasins B and D, and Colchicine on the Structure and Function of Thioglycolate-elicited Macrophages *

	Without PMA				With PMA (0.01 μg/ml)			
	Control	10^{-5} M CB+	10^{-5} M CD+	10^{-5} M Colchicine	Control	10^{-5} M CB	10^{-5} M CD	10^{-5} M Colchicine
Morphology	Spread	Round and arborized	Round and arborized	Round	Highly spread	Highly spread	Highly arborized	Highly spread
Surface area, μm^2	920	720	ND+	640	3120	2360	ND	1860
Pinocytosis, %	100	86	45	70	200-340	100	66	90
Microtubules in the peripheral cytoplasm	Present	Present	Present	None	Many	Many	Many	None
10-nm Filaments in the peripheral cytoplasm, % of cells	<5	<5	<5	None	57-63	Many	Many	None
Linear arrays of lysosomes, % of cells	<6	<6	ND	None	45-71	49	55	None
Actin-rich patches	None	None	None	None	Many	Few	None	Many

* Data from reference 25 and this report.

+ *CB*, cytochalasin B; *CD*, cytochalasin D; *ND*, not done.

Effects of PMA on Cytochalasin-sensitive Cytoskeletal Elements

PMA promotes cellular spreading (25) and the appearance of actin-rich patches at the basal surfaces of resident and thioglycolate-elicited macrophages (Fig. 3 *b* and *d*). (Similar patches containing α-actinin have been observed in fibroblasts at the points anchoring the cell to the substrate [19].) Colchicine has only a modest inhibitory effect of PMA-induced cell spreading (Table IV and reference 25), and neither colchicine nor podophyllotoxin prevents the PMA-induced formation of actin-rich patches (Fig. 3 *e* and *f*). These results indicate that microtubule and 10-nm filament extension are not required for macrophage spreading or for the formation of actin-rich patches.

Cytochalasin B has little effect on PMA-induced cellular spreading (25) but does reduce the number of actin-rich patches at the cell's basal surface. In contrast, cytochalasins D and E markedly inhibit cellular spreading in response to PMA (Figs. 7 *b* and 10 *c*). Microtubules and 10-nm filaments remain extended in thioglycolate macrophages treated with PMA and cytochalasin D or E. For this reason, the macrophages develop a "spiderlike" appearance (Fig. 7 *b* and 10 *c*) and exhibit narrow pseudopods filled with microtubules and 10-nm filaments radiating from the cytocenter.

The relative effectiveness of the several cytochalasins in inhibiting spreading (as opposed to pseudopod extension) in PMA-treated macrophages corresponds to the relative potencies of these drugs in inhibiting actin filament assembly (3, 20). These findings suggest that functional integrity of the actin filament system is required for PMA-stimulated cellular spreading to occur.

Colchicine- and Cytochalasin-sensitive Cytoskeletal Elements Function Independently of One Another

PMA-induced microtubule redistribution, 10-nm filament extension, and organelle movement are largely unaffected by cytochalasins D or B (Tables III and IV), whereas PMA-induced macrophage spreading occurs in the presence of colchicine, podophyllotoxin, vincristine, and vinblastine (25). Thus it seems likely that PMA stimulates each of these cytoplasmic processes independently of the other, and that the cytoskeletal elements that regulate them function independently of one another. Hoffstein and Weissmann (14) have come to similar conclusions from their studies of calcium ionophore–stimulated secretion of lysosomal enzymes in cytochalasin B–treated polymorphonuclear leukocytes.

Effects of Cytoskeletal Inhibitors on PMA-stimulated Pinocytosis

The most intriguing and least easily understood result of these studies is that both colchicine and the cytochalasins inhibit PMA-stimulated pinocytosis. We propose the following hypothesis to explain these findings. Plasma membrane movement, be it involved in cell spreading or phagocytosis, appears to be dependent upon the functional integrity of the actin filament system. Cytochalasin D, a potent inhibitor of macrophage spreading (see reference 25, Fig. 7 *b*, and Table IV), phagocytosis, and PMA-induced actin patch formation (see legend to Fig. 3), inhibits both basal-level (45% of control) and PMA-stimulated pinocytosis (25). (The failure of cytochalasin B to inhibit basal-level pinocytosis probably reflects its relative impotence [3, 20], compared to cytochalasin D, as an inhibitor of actin filament formation.) Taken together, these results suggest that the formation of pinocytic vacuoles is dependent upon actin filaments and that the cytochalasins inhibit PMA-stimulated pinocytosis by disrupting actin filaments at sites of plasma membrane internalization.

PMA-stimulated thioglycolate macrophages pinocytose an area of plasma membrane equivalent to their entire surface area every 14–20 min (25). Most of this internalized membrane appears to be recycled back to the cell surface (7, 24, 28, 29). Clearly, the rate at which membrane can be recycled must be related to the speed of pinosome translocation of lysosomes and the efficiency of return of this membrane to the cell surface. Colchicine-sensitive structures govern organelle movement in a variety of cellular systems. It is possible that agents that disrupt microtubules and inhibit 10-nm filament function slow membrane recycling and thereby limit the rate of pino-

cytosis. Viewed in this way, pinocytosis resembles a metabolic pathway. Coordination between the various steps in the pathway is necessary to achieve optimal efficiency. We suggest that the cytochalasins inhibit the membrane internalization step, whereas colchicine slows membrane recycling and retrieval.

Received for publication 26 October 1979, and in revised form 24 March 1980.

REFERENCES

1. Atlas, S. J., and S. Lin. 1978. Dihydrocytochalasin B. *J. Cell Biol.* 76:360–370.
2. Bikle, D., L. G. Tilney, and K. R. Porter. 1966. Microtubules and pigment migration in the melanophores of *Fundulus heteroclitus*. *J. Protoplasm.* 61:322–345.
3. Brenner, S. L., and E. D. Korn. 1979. Substoichiometric concentrations of cytochalasin D inhibit actin polymerization. *J. Biol. Chem.* 254:9982–9985.
4. Cohn, Z. A., and B. Benson. 1965. The differentiation of mononuclear phagocytes. Morphology, cytochemistry and biochemistry. *J. Exp. Med.* 121:1953–1970.
5. Dahlstrom, A. 1968. Effects of colchicine on transport of amine storage granules in sympathetic nerves of rat. *Eur. J. Pharmacol.* 5:111–113.
6. Eagle, H. 1959. Amino acid metabolism in mammalian cell cultures. *Science (Wash. D. C.).* 130:432–437.
7. Farquhar, M. G. 1978. Traffic of products and membranes through the Golgi complex. *In* Transport of Macromolecules in Cellular Systems. S. C. Silverstein, editor. Dahlem Konferenzen, Berlin. 341–362.
8. Goldman, R. D. 1971. The role of three cytoplasmic fibers in BHK-21 cell motility. I. Microtubules and the effects of colchicine. *J. Cell Biol.* 51:752–762.
9. Goldstein, I. M., S. T. Hoffstein, and G. Weissmann. 1975. Mechanisms of lysosomal enzyme release from human polymorphonuclear leukocytes. *J. Cell Biol.* 66:647–652.
10. Graham, R. C., and M. J. Karnovsky. 1966. The early stages of observation of injected horseradish peroxidase in the proximal tubules of mouse kidney: Ultrastructural cytochemistry by a new technique. *J. Histochem. Cytochem.* 14:291–302.
11. Griffin, F. M., Jr., J. A. Griffin, and S. C. Silverstein. 1976. Studies on the mechanism of phagocytosis. II. The interaction of macrophages with anti-immunoglobulin IgG-coated bone marrow-derived lymphocytes. *J. Exp. Med.* 144:788–809.
12. Hartwig, J. H., and T. P. Stossel. Interaction of actin, myosin, and an actin-binding protein of rabbit pulmonary macrophages. II. Effects of cytochalasin B. *J. Cell Biol.* 71:295–303.
13. Heletjaris, T. G., P. S. Lombardi, and L. A. Glasgow. 1976. Effect of cytochalasin B on the adhesion of mouse peritoneal macrophages. *J. Cell. Biol.* 69:407–414.
14. Hoffstein, S., and G. Weissmann. 1978. Microfilaments and microtubules in calcium ionophore-induced secretion of lysosomal enzymes from human polymorphonuclear leukocytes. *J. Cell Biol.* 78:769–781.
15. Holmes, K. V., and P. W. Choppin. 1968. On the role of microtubules in movement and alignment of nuclei in virus-induced syncytia. *J. Cell Biol.* 39:526–543.
16. Junqueira, L. C., and K. R. Porter. 1969. Mechanism for pigment migration in melanophores and erythrophores. *J. Cell Biol.* 43 (2, Pt. 2):62 *a* (Abstr.).
17. Karsson, J. O., H. A. Hanson, and J. Sjostrand. 1971. Effect of colchicine on axonal transport and morphology of retinal ganglion cells. *Z. Zellforsch. Mikrosk, Anat.* 115:265–283.
18. Kreutzberg, G. 1969. Neuronal dynamic and axonal flow. IV. Blockage of intraaxonal enzyme transport by colchicine. *Proc. Natl. Acad. Sci. U. S. A.* 62:722.
19. Lazarides, E. 1976. Aspects of the structural organization of actin filaments in tissue culture cells. *In* Cell Motility. R. Goldman, T. Pollard, and J. Rosenbaum, editors. Cold Spring Harbor Laboratory, Cold Spring Harbor, New York. 347–360.
20. Lin, D. C., K. D. Tobin, M. Gurmet, and S. Lin. 1980. Cytochalasins inhibit nuclei-induced actin polymerization by blocking filament elongation. *J. Cell Biol.* 84:455–460.
21. Locke, M., and N. Krishnan. 1971. Hot alcoholic phosphotungstic acid and uranyl acetate as routine stains for thick and thin sections. *J. Cell Biol.* 50:550–557.
22. Loike, J., and S. B. Horwitz. 1976. The effects of podophyllotoxin and VP-16-213 on microtubule assembly *in vitro* and nucleoside transport in HeLa cells. *Biochemistry.* 15: 5435–2442.
23. Luft, J. H. 1961. Improvements in epoxy resin embedding method. *J. Biophys. Biochem. Cytol.* 9:409–414.
24. Muller, W. A., R. M. Steinman, and Z. A. Cohn. 1979. Recycling of phagolysosome membrane proteins in cultured macrophages. *J. Cell Biol.* 83(2, Pt. 2)258 *a*. (Abstr.).
25. Phaire-Washington, L., E. Wang, and S. C. Silverstein. 1980. Phorbol myristate acetate stimulates pinocytosis and membrane spreading in mouse peritoneal macrophages. *J. Cell Biol.* 86:634–640.
26. Reynold, R. 1963. The use of lead citrate at high pH as an electron opaque stain in electron microscopy. *J. Cell Biol.* 17:208–212.
27. Rifkin, D. B., R. M. Crowe, and R. Pollack. 1979. Tumor promoters induce changes in chick embryo fibroblast cytoskeleton. *Cell.* 18:361–368.
28. Schneider, Y.-J., P. Tulkens, C. de Duve, and A. Trouet. 1979. Fate of plasma membrane during endocytosis. II. Evidence for recycling (shuttle) of plasma membrane constituents. *J. Cell Biol.* 82:449–465.
29. Silverstein, S. C., R. Steinman, and Z. A. Cohn. 1977. Endocytosis. *Annu. Rev. Biochem.* 46:669–722.
30. Snyder, J. A., and J. R. McIntosh. 1976. Biochemistry and physiology of microtubules. *Annu. Rev. Biochem.* 45:699–720.
31. Starger, J. M., W. E. Brown, A. E. Goldman, and R. D. Goldman. 1978. Biochemical and immunological analysis of rapidly purified 10-nm filaments from baby hamster kidney (BHK-21) cells. *J. Cell Biol.* 78:93–109.
32. Steinman, R. M., S. E. Brodie, and Z. A. Cohn. 1976. Membrane flow during pinocytosis. A stereological analysis. *J. Cell. Biol.* 68:665–687.
33. Tilney, L. G., and K. R. Porter. 1967. Studies on the microtubules in Heliozoa. II. The effect of low temperature on these structures in the formation and maintenance of axopodia. *J. Cell Biol.* 34:327–343.
34. Wang, E., R. K. Cross, and P. W. Choppin. 1979. The involvement of microtubules and 10-nm filaments in the movement and positioning of nuclei in syncytia. *J. Cell Biol.* 83: 320–337.
35. Wang, E., and A. R. Goldberg. 1978. Binding of deoxyribonuclease to actin. I. A new way to visualize microfilament bundles in nonmuscle cells. *J. Histochem. Cytochem.* 25:745–749.
36. Wang, E., and R. D. Goldman. 1978. Functions of cytoplasmic fibers in intracellular movements in BHK-21 cells. *J. Cell Biol.* 79:708–726.
37. Wang, E., and S. C. Silverstein. 1979. The distribution of 10-nm filaments and lysosomes in phorbol myristate acetate treated mouse peritoneal macrophages. *J. Cell Biol.* 83(2,Pt.2): 261 *a* (Abstr.).
38. Weihing, R. R. 1976. Cytochalasin B inhibits actin-related gelation of HeLa cell extracts. *J. Cell Biol.* 71:303–307.